

Corneal Biomechanical Metrics and Anterior Segment Parameters in Mild Keratoconus

Bruno M. Fontes, MD,^{1,2,3} Renato Ambrósio, Jr, MD, PhD,^{3,4} Daniela Jardim, MD,⁴ Guillermo C. Velarde, DSc,⁵ Walton Nosé, MD¹

Purpose: To compare corneal hysteresis (CH), corneal resistance factor (CRF), spherical equivalent (SE), average central keratometry (K-Avg), corneal astigmatism (CA), corneal volume (CV), anterior chamber (AC) depth, and central corneal thickness (CCT) between patients with mild keratoconus and healthy controls and to estimate the sensitivity and specificity of CH and CRF in discriminating mild keratoconus from healthy corneas.

Design: Comparative case series.

Participants: Sixty-three eyes (40 patients) with mild keratoconus (group 1) and 80 eyes from 40 gender- and age-matched controls (group 2).

Methods: Patients underwent a complete clinical eye examination, corneal topography (Humphrey ATLAS; Carl Zeiss Meditec, Dublin, CA), tomography (Pentacam; Oculus, Wetzlar, Germany), and biomechanical evaluations (ocular response analyzer; Reichert Ophthalmic Instruments, Depew, NY). The receiver operating characteristic (ROC) curve was used to identify cutoff points that maximized sensitivity and specificity in discriminating mild keratoconus from normal corneas.

Main Outcome Measures: Corneal hysteresis, CRF, SE, K-Avg, CA, CV, AC depth, and CCT. The diagnostic performance of CH and CRF for detecting mild keratoconus was assessed using the ROC curve.

Results: In group 1 versus group 2, the SE values (mean ± standard deviation) were -3.55 ± 2.87 diopters (D) versus -1.46 ± 3.09 D ($P = 0$); K-Avg, 45.09 ± 2.24 versus 43.24 ± 1.54 D ($P = 0$); CA, 3.15 ± 1.87 versus 1.07 ± 0.83 D ($P = 0$); CV, 57.3 ± 2.12 versus 60.86 ± 3.39 mm³ ($P = 0$); AC depth, 3.19 ± 0.35 versus 3.05 ± 0.43 mm ($P = 0.0416$); CCT, 503 ± 34.15 versus 544.71 ± 35.89 μm ($P = 0$); CH, 8.50 ± 1.36 versus 10.17 ± 1.79 mmHg ($P = 0$); CRF, 7.85 ± 1.49 versus 10.13 ± 2.0 mmHg ($P = 0$). The ROC curve analyses showed a poor overall predictive accuracy of CH (cutoff, 9.64 mmHg; sensitivity, 87%; specificity, 65%; test accuracy, 74.83%) and CRF (cutoff, 9.60 mmHg; sensitivity, 90.5%; specificity, 66%; test accuracy, 76.97%) for detecting mild keratoconus.

Conclusions: The values for CH, CRF, CV, and CCT were statistically lower and those for SE, K-Avg, CA, and AC depth were statistically higher in patients with mild keratoconus compared with controls. Corneal hysteresis and CRF were poor parameters for discriminating between mild keratoconus and normal corneas.

Financial Disclosure(s): Proprietary or commercial disclosure may be found after the references. *Ophthalmology* 2010;117:673–679 © 2010 by the American Academy of Ophthalmology.

Keratoconus is an ectatic, noninflammatory disorder in which corneal thinning and protrusion cause the cornea to assume a conical shape. It most commonly is bilateral and asymmetric, with no gender or race predilection, and begins typically at puberty.^{1–8} Detection of initial (mild) and sub-clinical (forme fruste) keratoconus is of paramount importance in the preoperative evaluation of refractive surgery candidates to avoid complications such as post-LASIK ectasia.^{9–12} New corneal imaging technologies and indices were described recently, and further research is underway.^{13–27}

Since the time Luce²⁸ developed the ocular response analyzer (ORA; Reichert Ophthalmic Instruments, Depew, NY), there has been increased interest in evaluating corneal biomechanics evaluation *in vivo*. The ORA records corneal inward and outward applanation after delivering a metered collimated air pulse and provides an indication of the viscosity and elastic properties of the cornea. Corneal hysteresis (CH) and corneal resistance factor (CRF), which are the corneal biomechanical metrics given by the ORA, have been the subjects of several recent publications.^{29–54} Cor-

neal biomechanical metrics may have great value in the preoperative screening of refractive surgery candidates, helping to differentiate between healthy and abnormal corneas.

This study compared anterior segment parameters, CH, and CRF between patients with mild keratoconus and control healthy subjects. The sensitivity and specificity of corneal biomechanical metrics for discriminating between mild keratoconus and normal corneas also were estimated.

Patients and Methods

The study constituted a comparative case series. The research followed the tenets of the Declaration of Helsinki and was approved by the ethics committee of the Federal University of São Paulo, Brazil (protocol 0123/06). All subjects were told of the purpose of the study and gave informed consent before inclusion. Patients were evaluated sequentially from October 2005 through December 2008. Demographic and clinical data were obtained, including date of birth, gender, and self-reported race or ethnicity.

Table 1. Keratoconus Grading Scheme

	Normal	Mild Keratoconus
Corneal topography	Regular axial topography pattern (round, oval, symmetric bow tie, etc.)	Axial topography consistent with keratoconus (increased area of corneal power surrounded by concentric areas of decreasing power, inferosuperior power asymmetry, or skewing of the steepest radial axes above and below the horizontal meridian) and flat keratometry reading <51.00 D
Slit-lamp examination	Normal	Fleischer ring or Vogt striae
Visual acuity	Spectacle-corrected acuity ≥ 55 letters at 4 m on logMAR chart (with no other ocular pathologic features)	Reduced spectacle-corrected acuity (<55 letters at 4 m on logMAR chart with no other ocular pathologic features)

D = diopters; logMAR = logarithm of the minimum angle of resolution. Adapted from McMahon et al.⁵

Each subject underwent a comprehensive ophthalmologic examination, which included a medical history review, best-corrected visual acuity, slit-lamp and fundoscopic examinations, Placido disc topography (Humphrey ATLAS; Carl Zeiss Meditec, Dublin, CA), Pentacam tomographic evaluation (Oculus, Wetzlar, Germany), and ORA measurements (Reichert Ophthalmic Instruments).

Mild keratoconus was defined using the grading scheme of the Collaborative Longitudinal Evaluation of Keratoconus Study Group⁵ (Table 1). The criteria were axial topography consistent with keratoconus, which includes an increased area of corneal power surrounded by concentric areas of decreasing power, inferior–superior power asymmetry, and skewing of the steepest radial axes above and below the horizontal meridian; a flat keratometry reading of less than 51.00 diopters (D); Fleischer ring or Vogt striae; no corneal scarring; and reduced spectacle acuity (with no other ocular pathologic features).

Cases were matched for gender and age with healthy subjects as controls. The subjects were divided in 2 groups: mild keratoconus (group 1) and control healthy eyes (group 2) for data comparison. Participant exclusion criteria were age younger than 18 years, any previous corneal or ocular surgery, any eye disease other than keratoconus, chronic or continuous use of topical medications, corneal scars or opacities, and declining informed consent. Contact lenses had to be removed at least 72 hours before the examination.

The patients underwent a clinical evaluation and testing with an ORA, corneal topography, and Pentacam tomography, all of which were performed by 2 trained ophthalmologists (RA and DJ) during the same visit. All measurements were obtained between 8 AM and 6 PM. Two consecutive ORA measurements were obtained from both eyes (only good-quality readings, as defined by the manufacturer, were stored), and the results were averaged. The spherical equivalent was obtained by dynamic refraction during the clinical examination. The average central keratometry, central corneal thickness, corneal volume, corneal astigmatism, and anterior chamber depth were assessed using the Pentacam system.

The Pentacam system was connected to a personal computer with automated software. The device had been calibrated by the manufacturer. The system uses a rotating Scheimpflug camera and a monochromatic slit light source (blue LED at 475 nm) that rotate together around the optical axis of the eye. After proper alignment of the face, the patient is shown a target to guide fixation. The examiner sees a real-time image of the patient's eye on the computer screen, and the image is focused and centered manually. The rotating camera was set to take 25 slit images of the anterior eye segment in approximately 2 seconds with 500 true elevation points incorporated into each slit image. Minute eye movements were

captured by a second camera and were corrected simultaneously. Single-point pachymetric measurements of the entire cornea were determined by separating of the calculated front and back corneal surfaces. All data were measured in each of the single images of a scan, giving very accurate and precise values.^{14,15,18,24,25,55}

An ORA determines corneal biomechanical properties using an applied force-displacement relationship, and the details have been described previously.^{28,35,44–46,48,49,56–62} Briefly, a precisely metered air pulse is delivered to the eye, causing the cornea to move inward, past applanation, and into slight concavity. Milliseconds after the initial applanation, the air pump generating the air pulse is shut off and the pressure applied to the eye decreases in an inverse-time, symmetrical fashion. As the pressure decreases, the cornea passes through a second applanated state while returning from concavity to its normal convex curvature. Energy adsorption during rapid corneal deformation delays the occurrence of the inward and outward applanation signal peaks, resulting in a difference between the applanation pressures. The difference between these inward and outward motion applanation pressures is the CH and is an indication of viscous damping in the cornea, reflecting the capacity of corneal tissue to absorb and dissipate energy. Corneal resistance factor is a measure of the cumulative effects of both the viscous and elastic resistance encountered by the air jet while deforming the corneal surface; it is an indicator of the overall resistance of the cornea. The CRF was derived empirically to maximize the correlation with the central corneal thickness (Luce D. Methodology for cornea compensated IOP and CRF for the Reichert ocular response analyzer. Invest Ophthalmol Vis Sci 2006;47:E-Abstract 2266), and it can be considered as weighted by the elastic resistance because of its stronger correlation with central corneal thickness than with CH. Although CH and CRF are related, they can differ significantly in some instances, and each provides distinct information about the cornea.

The receiver operating characteristic (ROC) curve was used to identify the best CH and CRF cutoff points to maximize the sensitivity and specificity for discriminating mild keratoconus from normal corneas. The ROC curve was obtained by plotting sensitivity against 1–specificity, calculated for each value observed. Ideally, an area of 100% implies that the test perfectly discriminates between groups. Logistic regression was used to support the cutoff point identified in the ROC curve analysis.

The cases were gender- and age-matched with control subjects for data comparison, because relationships between these 2 variables with CH and CRF were found previously.⁵² Data are expressed as the mean \pm standard deviation.

Table 2. Summary Data from the Studied Population

	Group 1: Mild Keratoconus	Group 2: Control	Statistical Analysis
Male/female	18/22	18/22	
Mean age±SD (range), yrs	34.98±12.4 (18–73)	35.23±12.6 (18–72)	$P = 1$
Spherical equivalent (range), D	-3.55±2.87 (-10.25 to 3.75)	-1.46±3.09 (-9.25 to 8.00)	$P = 0^*$
Average central keratometry (range), D	45.09±2.24 (40.40–50.85)	43.24±1.54 (39.90–46.75)	$P = 0^†$ (95% CI, -2.48 to -1.23)
Corneal astigmatism (range), D	3.15±1.87 (0.70–9.50)	1.07±0.83 (0–4.90)	$P = 0^*$
Anterior chamber depth (range), mm	3.19±0.35 (2.41–5.21)	3.05±0.43 (2.08–3.80)	$P = 0.0416^†$ (95% CI, -0.27 to -0.01)
Corneal volume (range), mm ³	57.3±2.12 (49.5–66.9)	60.86±3.39 (53.7–68.5)	$P = 0^†$ (95% CI, -4.45 to -2.21)
Central corneal thickness (range), μm	503±34.15 (414–568)	544.71±35.89 (457–627)	$P = 0^†$ (95% CI, 30.01–53.41)
Corneal hysteresis (range), mmHg	8.50±1.36 (5.71–11.80)	10.17±1.79 (5.95–14.58)	$P = 0^†$ (95% CI, 1.13–2.20)
Corneal resistance factor (range), mmHg	7.85±1.49 (5.01–11.20)	10.13±2.0 (5.45–15.10)	$P = 0^†$ (95% CI, 1.68–2.88)

CI = confidence interval; D = diopters; SD = standard deviation.

Data are expressed as mean±standard deviation (where applied).

*Wilcoxon rank-sum test.

†Standard 2-sample *t* test.

Results

Group 1 consisted of 63 eyes from 40 patients with mild keratoconus (defined in Table 1). Group 2 included 80 eyes from 40 healthy participants, who were gender- and age-matched with the cases. Each group comprised 18 females and 22 males. The mean age±standard deviation was 34.98±12.4 years in group 1 and 35.23±12.6 years in group 2. The results are summarized in Table 2.

The spherical equivalent was -3.55±2.87 D (range, -10.25 to 3.75 D) in group 1 and -1.46±3.09 D (-9.25 to 8.00 D) in group 2 ($P = 0$, Wilcoxon rank-sum test). The average central keratometry values were 45.09±2.24 D (range, 40.40–50.85 D) and 43.24±1.54 D (range, 39.90–46.75 D) in groups 1 and 2, respectively ($P = 0$; 95% confidence interval, -2.48 to -1.23; standard 2-sample *t* test). Corneal astigmatism (given by corneal topography) was significantly higher in group 1 (mean, 3.15±1.87 D; range, 0.70–9.50 D) than in group 2 (1.07±0.83 D; range, 0–4.90 D; $P = 0$, Wilcoxon rank-sum test).

The corneal volume was 57.3±2.12 mm³ (range, 49.5–66.9 mm³) in group 1 and 60.86±3.39 mm³ (range, 53.7–68.5 mm³) in group 2 ($P = 0$; 95% confidence interval, -4.45 to -2.21; standard 2-sample *t* test). Anterior chamber depth was significantly greater in group 1 (mean, 3.19±0.35 mm; range, 2.41–5.21 mm) com-

pared with that of group 2 (mean, 3.05±0.43 mm; range, 2.08–3.80 mm; $P = 0.0416$; 95% confidence interval, -0.27 to -0.01; standard 2-sample *t* test). The central corneal thickness measurements were 503±34.15 μm (range, 414–568 μm) and 544.71±35.89 μm (457–627 μm) in groups 1 and 2, respectively ($P = 0$; 95% confidence interval, 30.01–53.41; standard 2-sample *t* test).

Corneal hysteresis was 8.50±1.36 mmHg (range, 5.71–11.80 mmHg) in group 1 and 10.17±1.79 mmHg (range, 5.95–14.58 mmHg) in group 2 ($P = 0$; 95% confidence interval, 1.13–2.20; standard 2-sample *t* test). The distribution of CH in each group is shown in Figure 1. Corneal resistance factor was 7.85±1.49 mmHg (range, 5.01–11.20 mmHg) and 10.13±2.0 mmHg (range, 5.45–15.10 mmHg) in groups 1 and 2, respectively ($P = 0$; 95% confidence interval, 1.68–2.88; standard 2-sample *t* test), and their distributions are shown in Figure 2.

The ROC curve analysis (Fig 3) showed a poor overall predictive accuracy of CH for detecting mild keratoconus. The optimal cutoff point was 9.64 mmHg, with 87% sensitivity and 65% specificity (test accuracy, 74.83%). The sensitivity and specificity of other CH cutoff points are shown in Table 3.

The ROC curve analysis (Fig 4) also showed a poor overall predictive accuracy of CRF for detecting mild keratoconus; the

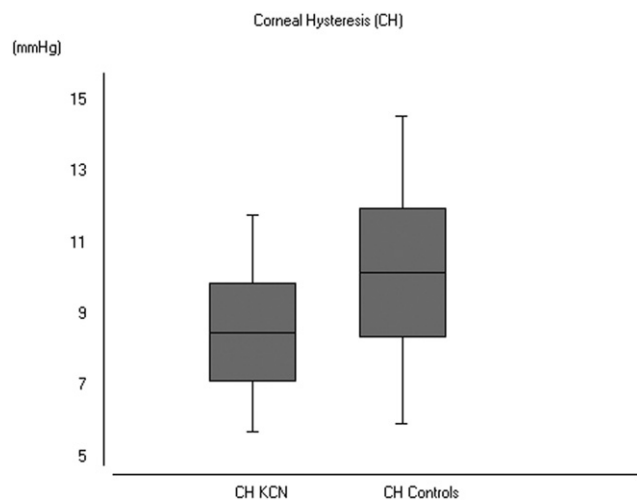


Figure 1. Box plot showing corneal hysteresis (CH) distribution in both groups. KCN = keratoconus.

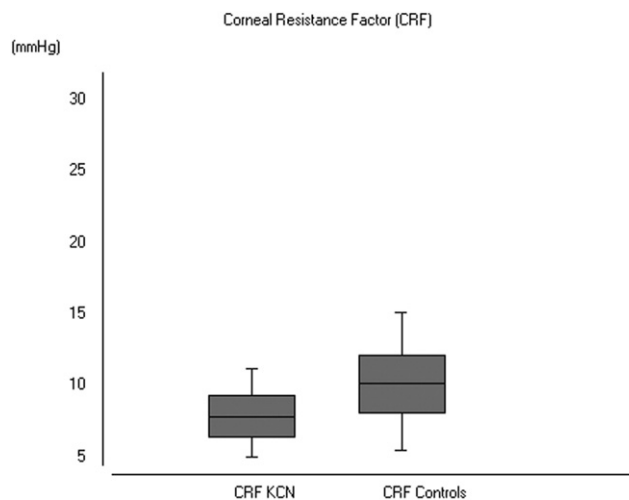


Figure 2. Box plot showing corneal resistance factor (CRF) distribution in both groups. KCN = keratoconus.

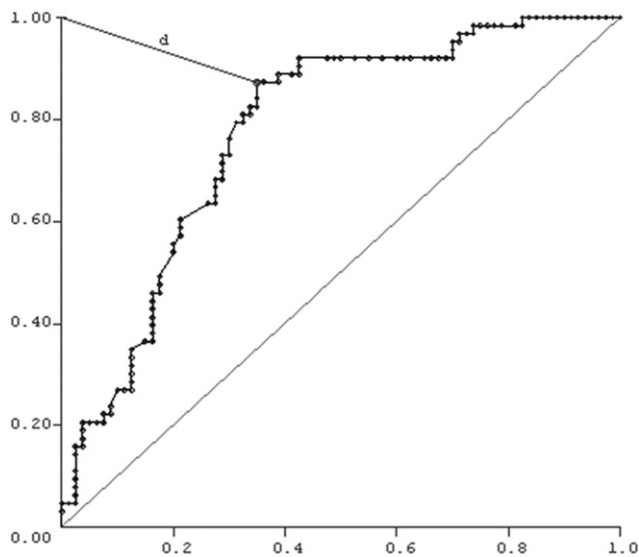


Figure 3. Receiver operating characteristic (ROC) curve (graphical plot of the sensitivity vs. 1-specificity) for corneal hysteresis (CH) data. The cutoff was 9.64 mmHg, with 87% sensitivity and 65% specificity (test accuracy, 74.83%). d = distance from cutoff point to the upper left corner or coordinate (0,1) of the ROC space (the best possible prediction point that represents 100% of sensitivity and specificity, also called a perfect classification).

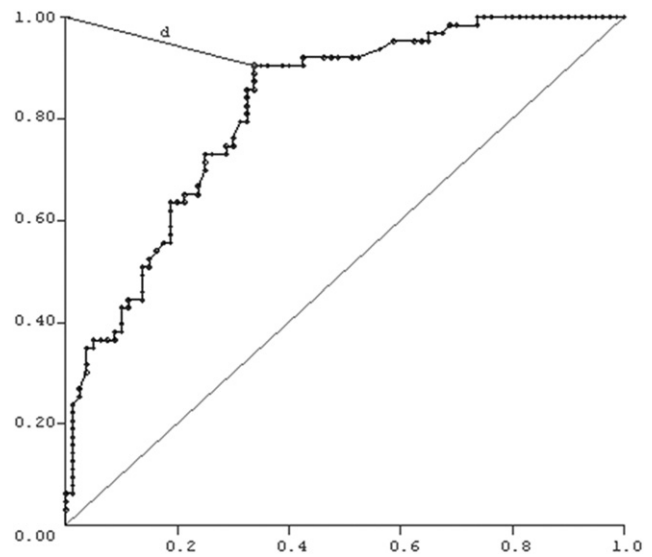


Figure 4. Receiver operating characteristic (ROC) curve (graphical plot of the sensitivity vs. 1-specificity) for corneal resistance factor (CRF) data. The cutoff was 9.60 mmHg, with 90.5% sensitivity and 66% specificity (test accuracy, 76.97%). d = distance from cutoff point to the upper left corner or coordinate (0,1) of the ROC space (the best possible prediction point that represents 100% of sensitivity and specificity, also called a perfect classification).

best cutoff point was 9.60 mmHg, with 90.5% sensitivity and 66% specificity (test accuracy, 76.97%). The sensitivity and specificity of other CRF cutoff points are shown in Table 4.

Discussion

The ability to detect mild and subclinical (forme fruste) forms of keratoconus has improved greatly in recent years. Although Placido disc-based corneal topography remains the most widely used tool, new tomographic indices such as corneal pachymetric progression and elevation analysis have helped in identifying subtle abnormalities in corneal anatomic

features.^{3,9,15,16,18,22,23,25,27,63,64} Nevertheless, new cases of corneal ectasia occurring after refractive surgery still are reported quite often.^{9-12,65} A test that could classify the corneal biomechanical strength consistently to predict the response after surgery would have great usefulness.

Healthy human corneal tissue is composed mainly of heterotypic collagen type I fibrils and is an anisotropic, biocomposite structure with high tensile strength that provides the globe with a resilient layer.⁶⁶⁻⁷² It is considered a viscoelastic material with measurable properties.^{28,37,46,48,52,62,70,73-77} In a pioneering study, Luce²⁸ proposed that CH, determined using an ocular response analyzer, could be an independent indicator or corneal biomechanical measurement in vivo, with probable practical applications in

Table 3. Sensitivity and Specificity for Different Cutoff Points of Corneal Hysteresis

Mild Keratoconus vs. Controls		
Cutoff Point (mmHg)	Sensitivity (%)	Specificity (%)
CH≤7.0	16	98
CH≤7.5	22	91
CH≤8.0	35	88
CH≤8.25	35	84
CH≤8.5	46	84
CH≤8.75	57	79
CH≤9.0	67	73
CH≤9.25	73	70
CH≤9.5	79	66
CH≤9.75	89	58
CH≤10	92	58

CH = corneal hysteresis.

Table 4. Sensitivity and Specificity for Different Cutoff Points of Corneal Resistance Factor

Mild Keratoconus vs. Controls		
Cutoff Point (mmHg)	Sensitivity (%)	Specificity (%)
CRF≤7.0	35	95
CRF≤7.5	37	91
CRF≤8.0	49	86
CRF≤8.25	59	81
CRF≤8.5	65	76
CRF≤8.75	73	71
CRF≤9.0	79	70
CRF≤9.25	83	68
CRF≤9.5	89	66
CRF≤9.75	90	61
CRF≤10	92	49

CRF = corneal resistance factor.

preoperative screening for refractive surgery. Several studies have reported interesting results for refractive surgery candidates as well as for healthy persons and those with glaucoma or ectasia.^{28–32,34–49,51–54,56–62,66,73–75,78–85}

Previously, the authors' group found that both CH and CRF had a negative relationship with age, a positive relationship with corneal thickness, and no correlation with spherical equivalent, anterior chamber depth, or central keratometry.⁵² An ongoing study is being conducted with pachymetry-matched subjects to determine whether ORA helps to differentiate abnormalities such as thin or thick corneas in special cases. In addition, Luce presented new data (Luce D. ORA Waveform Analysis and beyond. Presented at: American Society of Cataract and Refractive Surgery Annual Meeting, April 3–8, 2009; San Francisco, California) regarding waveform parameters provided from the ORA signal that may be more sensitive than CH or CRF in discriminating abnormal corneas.

In this study, the corneal biomechanical metrics were statistically lower in patients with mild keratoconus compared with those in healthy controls. However, no cutoff value could be established with high sensitivity and specificity for the diagnosis of mild keratoconus, based on the diagnosis determined with Placido disc-based corneal topography. As expected, the spherical equivalent measurements revealed that the keratoconic patients were significantly more myopic than the control subjects. Keratoconic patients also had significantly steeper corneas of less volume and significantly higher corneal astigmatism, based on the central keratometric, corneal volume, and corneal astigmatism measurements. In addition, the central corneal thickness was statistically lower in the mild keratoconus group compared with the control group. An interesting finding was the difference in anterior chamber depth, showing that corneal protrusion makes the anterior chamber wider in keratoconus patients compared with normal subjects.

Corneal biomechanical metrics may prove to be useful for the preoperative screening of refractive surgery candidates and may help clinicians choose between surface ablation techniques such as photorefractive keratectomy and incisional procedures such as LASIK. Based on the present findings, CH and CRF should not be used as the sole criteria in the diagnosis of mild keratoconus. Additional research on this new technology is warranted to elucidate its full usefulness in daily practice.

References

- Shirayama-Suzuki M, Amano S, Honda N, et al. Longitudinal analysis of corneal topography in suspected keratoconus. *Br J Ophthalmol* 2009;93:815–9.
- Reeves SW, Ellwein LB, Kim T, et al. Keratoconus in the Medicare population. *Cornea* 2009;28:40–2.
- Li Y, Meisler DM, Tang M, et al. Keratoconus diagnosis with optical coherence tomography pachymetry mapping. *Ophthalmology* 2008;115:2159–66.
- Belin MW, Khachikian SS. Keratoconus: it is hard to define, but . . . *Am J Ophthalmol* 2007;143:500–3.
- McMahon TT, Szczołka-Flynn L, Barr JT, et al. CLEK Study Group. A new method for grading the severity of keratoconus: the Keratoconus Severity Score (KSS). *Cornea* 2006;25:794–800.
- Rabinowitz YS. Keratoconus. *Surv Ophthalmol* 1998;42:297–319.
- Rabinowitz YS, McDonnell PJ. Computer-assisted corneal topography in keratoconus. *Refract Corneal Surg* 1989;5:400–8.
- McGhee CN. 2008 Sir Norman McAlister Gregg Lecture: 150 years of practical observations on the conical cornea—what have we learned? *Clin Experiment Ophthalmol* 2009;37:160–76.
- Randleman JB. Post-laser in-situ keratomileusis ectasia: current understanding and future directions. *Curr Opin Ophthalmol* 2006;17:406–12.
- Rabinowitz YS. Ectasia after laser in situ keratomileusis. *Curr Opin Ophthalmol* 2006;17:421–6.
- Klein SR, Epstein RJ, Randleman JB, Stulting RD. Corneal ectasia after laser in situ keratomileusis in patients without apparent preoperative risk factors. *Cornea* 2006;25:388–403.
- Condon PI. 2005 ESCRS Ridley Medal Lecture: will keratectasia be a major complication for LASIK in the long term? *J Cataract Refract Surg* 2006;32:2124–32.
- Vinciguerra P, Albe E, Trazza S, et al. Refractive, topographic, tomographic, and aberrometric analysis of keratoconic eyes undergoing corneal cross-linking. *Ophthalmology* 2009;116:369–78.
- Prospero Ponce CM, Rocha KM, Smith SD, Krueger RR. Central and peripheral corneal thickness measured with optical coherence tomography, Scheimpflug imaging, and ultrasound pachymetry in normal, keratoconus-suspect, and post-laser in situ keratomileusis eyes. *J Cataract Refract Surg* 2009;35:1055–62.
- Pinero DP, Alio JL, Aleson A, et al. Pentacam posterior and anterior corneal aberrations in normal and keratoconic eyes. *Clin Exp Optom* 2009;92:297–303.
- Lema I, Romero P, Mato JL, Feijoo ED. Corneal descriptive indices in the fellow eye of unilateral keratoconus. *Eye Contact Lens* 2009;35:65–8.
- Khachikian SS, Belin MW. Posterior elevation in keratoconus [letter]. *Ophthalmology* 2009;116:816; author reply 816–7.
- Kawamorita T, Uozato H, Kamiya K, et al. Repeatability, reproducibility, and agreement characteristics of rotating Scheimpflug photography and scanning-slit corneal topography for corneal power measurement. *J Cataract Refract Surg* 2009;35:127–33.
- Belin MW, Khachikian SS. An introduction to understanding elevation-based topography: how elevation data are displayed—a review. *Clin Experiment Ophthalmol* 2009;37:14–29.
- McGhee CN, Altaie R. Assessing computerized tomography and higher-order aberration in the diagnosis of manifest and subclinical keratoconus. *Clin Experiment Ophthalmol* 2008;36:807–9.
- de Sanctis U, Loiacono C, Richiardi L, et al. Sensitivity and specificity of posterior corneal elevation measured by Pentacam in discriminating keratoconus/subclinical keratoconus. *Ophthalmology* 2008;115:1534–9.
- Swartz T, Marten L, Wang M. Measuring the cornea: the latest developments in corneal topography. *Curr Opin Ophthalmol* 2007;18:325–33.
- Konstantopoulos A, Hossain P, Anderson DF. Recent advances in ophthalmic anterior segment imaging: a new era for ophthalmic diagnosis? *Br J Ophthalmol* 2007;91:551–7.
- Emre S, Doganay S, Yologlu S. Evaluation of anterior segment parameters in keratoconic eyes measured with the Pentacam system. *J Cataract Refract Surg* 2007;33:1708–12.
- de Sanctis U, Missolungi A, Mutani B, et al. Reproducibility and repeatability of central corneal thickness measurement in

- keratoconus using the rotating Scheimpflug camera and ultrasound pachymetry. *Am J Ophthalmol* 2007;144:712–8.
26. Ucakhan OO, Ozkan M, Kanpolat A. Corneal thickness measurements in normal and keratoconic eyes: Pentacam comprehensive eye scanner versus noncontact specular microscopy and ultrasound pachymetry. *J Cataract Refract Surg* 2006;32:970–7.
 27. Ambrosio R Jr, Alonso RS, Luz A, Coca Velarde LG. Corneal-thickness spatial profile and corneal-volume distribution: tomographic indices to detect keratoconus. *J Cataract Refract Surg* 2006;32:1851–9.
 28. Luce DA. Determining in vivo biomechanical properties of the cornea with an ocular response analyzer. *J Cataract Refract Surg* 2005;31:156–62.
 29. Sun L, Shen M, Wang J, et al. Recovery of corneal hysteresis after reduction of intraocular pressure in chronic primary angle-closure glaucoma. *Am J Ophthalmol* 2009;147:1061–6.
 30. Shah S, Laiquzzaman M, Yeung I, et al. The use of the Ocular Response Analyser to determine corneal hysteresis in eyes before and after excimer laser refractive surgery. *Cont Lens Anterior Eye* 2009;32:123–8.
 31. Shah S, Laiquzzaman M. Comparison of corneal biomechanics in pre and post-refractive surgery and keratoconic eyes by Ocular Response Analyser. *Cont Lens Anterior Eye* 2009;32:129–32.
 32. Goldich Y, Barkana Y, Gerber Y, et al. Effect of diabetes mellitus on biomechanical parameters of the cornea. *J Cataract Refract Surg* 2009;35:715–9.
 33. Chen D, Lam AK, Cho P. A pilot study on the corneal biomechanical changes in short-term orthokeratology. *Ophthalmic Physiol Opt* 2009;29:464–71.
 34. Touboul D, Roberts C, Kerautret J, et al. Correlations between corneal hysteresis, intraocular pressure, and corneal central pachymetry. *J Cataract Refract Surg* 2008;34:616–22.
 35. Sullivan-Mee M, Billingsley SC, Patel AD, et al. Ocular Response Analyzer in subjects with and without glaucoma. *Optom Vis Sci* 2008;85:463–70.
 36. Song Y, Congdon N, Li L, et al. Corneal hysteresis and axial length among Chinese secondary school children: the Xichang Pediatric Refractive Error Study (X-PRES) report no. 4. *Am J Ophthalmol* 2008;145:819–26.
 37. Shen M, Wang J, Qu J, et al. Diurnal variation of ocular hysteresis, corneal thickness, and intraocular pressure. *Optom Vis Sci* 2008;85:1185–92.
 38. Shen M, Fan F, Xue A, et al. Biomechanical properties of the cornea in high myopia. *Vision Res* 2008;48:2167–71.
 39. Shah S, Laiquzzaman M, Mantry S, Cunliffe I. Ocular response analyser to assess hysteresis and corneal resistance factor in low tension, open angle glaucoma and ocular hypertension. *Clin Experiment Ophthalmol* 2008;36:508–13.
 40. Moreno-Montanes J, Maldonado MJ, Garcia N, et al. Reproducibility and clinical relevance of the ocular response analyzer in nonoperated eyes: corneal biomechanical and tonometric implications. *Invest Ophthalmol Vis Sci* 2008;49:968–74.
 41. Lim L, Gazzard G, Chan YH, et al. Cornea biomechanical characteristics and their correlates with refractive error in Singaporean children. *Invest Ophthalmol Vis Sci* 2008;49:3852–7.
 42. Kynigopoulos M, Schlote T, Kotecha A, et al. Repeatability of intraocular pressure and corneal biomechanical properties measurements by the ocular response analyser. *Klin Monatsbl Augenheilkd* 2008;225:357–60.
 43. Kucumen RB, Yenerel NM, Gorgun E, et al. Corneal biomechanical properties and intraocular pressure changes after phacoemulsification and intraocular lens implantation. *J Cataract Refract Surg* 2008;34:2096–8.
 44. Kirwan C, O'Malley D, O'Keefe M. Corneal hysteresis and corneal resistance factor in keratoectasia: findings using the Reichert ocular response analyzer. *Ophthalmologica* 2008;222:334–7.
 45. Kirwan C, O'Keefe M. Corneal hysteresis using the Reichert ocular response analyser: findings pre- and post-LASIK and LASEK. *Acta Ophthalmol* 2008;86:215–8.
 46. Kida T, Liu JH, Weinreb RN. Effects of aging on corneal biomechanical properties and their impact on 24-hour measurement of intraocular pressure. *Am J Ophthalmol* 2008;146:567–72.
 47. Kerautret J, Colin J, Touboul D, Roberts C. Biomechanical characteristics of the ectatic cornea. *J Cataract Refract Surg* 2008;34:510–3.
 48. Kamiya K, Hagishima M, Fujimura F, Shimizu K. Factors affecting corneal hysteresis in normal eyes. *Graefes Arch Clin Exp Ophthalmol* 2008;246:1491–4.
 49. Hoffer KJ. Corneal hysteresis and axial length among Chinese children [letter]. *Am J Ophthalmol* 2008;146:789; author reply 789.
 50. Gonzalez-Mejome JM, Villa-Collar C, Queiros A, et al. Pilot study on the influence of corneal biomechanical properties over the short term in response to corneal refractive therapy for myopia. *Cornea* 2008;27:421–6.
 51. Gonzalez-Mejome JM, Queiros A, Jorge J, et al. Intraoffice variability of corneal biomechanical parameters and intraocular pressure (IOP). *Optom Vis Sci* 2008;85:457–62.
 52. Fontes BM, Ambrosio R Jr, Alonso RS, et al. Corneal biomechanical metrics in eyes with refraction of -19.00 to $+9.00$ D in healthy Brazilian patients. *J Refract Surg* 2008;24:941–5.
 53. Elsheikh A, Wang D, Rama P, et al. Experimental assessment of human corneal hysteresis. *Curr Eye Res* 2008;33:205–13.
 54. Ehongo A, De Maertelaer V, Pourjavan S. Effect of topical corneal anaesthesia on ocular response analyzer parameters: pilot study. *Int Ophthalmol* 2009;29:325–8.
 55. Miranda MA, Radhakrishnan H, O'Donnell C. Repeatability of corneal thickness measured using an Oculus Pentacam. *Optom Vis Sci* 2009;86:266–72.
 56. Mollan SP, Wolffsohn JS, Nessim M, et al. Accuracy of Goldmann, ocular response analyser, Pascal and TonoPen XL tonometry in keratoconic and normal eyes. *Br J Ophthalmol* 2008;92:1661–5.
 57. Carbonaro F, Andrew T, Mackey DA, et al. The heritability of corneal hysteresis and ocular pulse amplitude: a twin study. *Ophthalmology* 2008;115:1545–9.
 58. Shah S, Laiquzzaman M, Bhojwani R, et al. Assessment of the biomechanical properties of the cornea with the ocular response analyzer in normal and keratoconic eyes. *Invest Ophthalmol Vis Sci* 2007;48:3026–31.
 59. Ortiz D, Pinero D, Shabayek MH, et al. Corneal biomechanical properties in normal, post-laser in situ keratomileusis, and keratoconic eyes. *J Cataract Refract Surg* 2007;33:1371–5.
 60. Gatinel D, Chaabouni S, Adam PA, et al. Corneal hysteresis, resistance factor, topography, and pachymetry after corneal lamellar flap. *J Refract Surg* 2007;23:76–84.
 61. Shah S, Laiquzzaman M, Cunliffe I, Mantry S. The use of the Reichert ocular response analyser to establish the relationship between ocular hysteresis, corneal resistance factor and central corneal thickness in normal eyes. *Cont Lens Anterior Eye* 2006;29:257–62.
 62. Kirwan C, O'Keefe M, Lanigan B. Corneal hysteresis and intraocular pressure measurement in children using the Reichert ocular response analyzer. *Am J Ophthalmol* 2006;142:990–2.

63. Steele TM, Fabinyi DC, Couper TA, Loughnan MS. Prevalence of Orbscan II corneal abnormalities in relatives of patients with keratoconus. *Clin Experiment Ophthalmol* 2008; 36:824–30.
64. Luz A, Ursulio M, Castaneda D, Ambrosio R Jr. Corneal thickness progression from the thinnest point to the limbus: study based on a normal and a keratoconus population to create reference values [in Portuguese]. *Arq Bras Oftalmol* 2006;69:579–83.
65. Wang JC, Hufnagel TJ, Buxton DF. Bilateral keratectasia after unilateral laser in situ keratomileusis: a retrospective diagnosis of ectatic corneal disorder. *J Cataract Refract Surg* 2003;29: 2015–8.
66. Kotecha A. What biomechanical properties of the cornea are relevant for the clinician? *Surv Ophthalmol* 2007;52(suppl): S109–14.
67. Stonecipher K, Ignacio TS, Stonecipher M. Advances in refractive surgery: microkeratome and femtosecond laser flap creation in relation to safety, efficacy, predictability, and biomechanical stability. *Curr Opin Ophthalmol* 2006;17:368–72.
68. Dupps WJ Jr, Wilson SE. Biomechanics and wound healing in the cornea. *Exp Eye Res* 2006;83:709–20.
69. Boote C, Hayes S, Abahussin M, Meek KM. Mapping collagen organization in the human cornea: left and right eyes are structurally distinct. *Invest Ophthalmol Vis Sci* 2006;47: 901–8.
70. Torres RM, Merayo-Llloves J, Jaramillo MA, Galvis V. Corneal biomechanics [in Spanish]. *Arch Soc Esp Oftalmol* 2005; 80:215–23.
71. Ethier CR, Johnson M, Ruberti J. Ocular biomechanics and biotransport. *Annu Rev Biomed Eng* 2004;6:249–73.
72. Ehlers N, Hjortdal J. Corneal thickness: measurement and implications. *Exp Eye Res* 2004;78:543–8.
73. Chen MC, Lee N, Bourla N, Hamilton DR. Corneal biomechanical measurements before and after laser in situ keratomileusis. *J Cataract Refract Surg* 2008;34:1886–91.
74. Pepose JS, Feigenbaum SK, Qazi MA, et al. Changes in corneal biomechanics and intraocular pressure following LASIK using static, dynamic, and noncontact tonometry. *Am J Ophthalmol* 2007;143:39–47.
75. Dupps WJ Jr. Hysteresis: new mechanospeak for the ophthalmologist. *J Cataract Refract Surg* 2007;33:1499–501.
76. Velten K, Gunther M, Oberacher-Velten I, Lorenz B. Finite-element simulation of corneal appplanation [letter]. *J Cataract Refract Surg* 2006;32:1073–4; author reply 1074.
77. Kohlhaas M, Spoerl E, Schilde T, et al. Biomechanical evidence of the distribution of cross-links in corneas treated with riboflavin and ultraviolet A light. *J Cataract Refract Surg* 2006;32:279–83.
78. Goldich Y, Barkana Y, Morad Y, et al. Can we measure corneal biomechanical changes after collagen cross-linking in eyes with keratoconus?—a pilot study. *Cornea* 2009;28:498–502.
79. del Buey MA, Cristobal JA, Ascaso FJ, et al. Biomechanical properties of the cornea in Fuchs' corneal dystrophy. *Invest Ophthalmol Vis Sci* 2009;50:3199–202.
80. Hager A, Loge K, Schroeder B, et al. Effect of central corneal thickness and corneal hysteresis on tonometry as measured by dynamic contour tonometry, ocular response analyzer, and Goldmann tonometry in glaucomatous eyes. *J Glaucoma* 2008;17:361–5.
81. Lam A, Chen D, Chiu R, Chui WS. Comparison of IOP measurements between ORA and GAT in normal Chinese. *Optom Vis Sci* 2007;84:909–14.
82. Hager A, Loge K, Fullhas MO, et al. Changes in corneal hysteresis after clear corneal cataract surgery. *Am J Ophthalmol* 2007;144:341–6.
83. Medeiros FA, Weinreb RN. Evaluation of the influence of corneal biomechanical properties on intraocular pressure measurements using the ocular response analyzer. *J Glaucoma* 2006;15:364–70.
84. Martinez-de-la-Casa JM, Garcia-Feijoo J, Fernandez-Vidal A, et al. Ocular response analyzer versus Goldmann applanation tonometry for intraocular pressure measurements. *Invest Ophthalmol Vis Sci* 2006;47:4410–4.
85. Laiquzzaman M, Bhojwani R, Cunliffe I, Shah S. Diurnal variation of ocular hysteresis in normal subjects: relevance in clinical context. *Clin Experiment Ophthalmol* 2006;34: 114–8.

Footnotes and Financial Disclosures

Originally received: February 23, 2009.

Final revision: August 29, 2009.

Accepted: September 14, 2009.

Available online: February 5, 2010.

Manuscript no. 2009-262.

¹ Department of Ophthalmology, Federal University of São Paulo, São Paulo, Brazil.

² Centro de Microcirurgia e Diagnóstico, Rio de Janeiro, Brazil.

³ REFRACTA—RIO, Rio de Janeiro, Brazil.

⁴ Renato Ambrósio Eye Institute, Rio de Janeiro, Brazil.

⁵ Fluminense Federal University, Rio de Janeiro, Brazil.

Financial Disclosure(s):

The author(s) have made the following disclosure(s):

R. Ambrósio - Consultant - Oculus and Reichert.

Correspondence:

Bruno M. Fontes, MD, Av. das Acacias 150 bl 2 apto 1001, Barra da Tijuca, Rio de Janeiro-RJ 22776-000, Brazil. E-mail: brunomfontes@terra.com.br.